Investigation of polarization-dependent interactions between optically-trapped colloidal microspheres

Aaron J. Lemmer
Univ. of Wisconsin-River Falls, Physics Dept.
River Falls, WI 54022

Colloidal systems have proven to be insightful models for many systems in soft condensed matter physics research, and when manipulated with optical tweezers, offer a platform for studies of both static and dynamic light-matter interactions. A pair of electronically-steerable optical traps was employed to control the position of dielectric microspheres suspended in aqueous solution, and dynamic trends in various system arrangements were examined. We study the behavior of particles in a three-dimensional line trap formed by a high-speed scanning mirror, and then implement this knowledge to realize a dynamic configuration of trapped particles that facilitates the isolation of polarization-dependent trap characteristics from scattering- and interference-related effects. Experimentation concerning observed polarization-dependent behavior is discussed, with previously-published theoretical descriptions and numerical simulations carefully considered.

I. INTRODUCTION

Optical micromanipulation, commonly manifested in the form of an optical tweezers, employs a single highly-focused Gaussian laser beam to generate an optical field gradient that attracts dielectric spheres of higher refractive index than their surrounding medium to the field maximum in all three spatial dimensions. The use of light-matter interactions in this manner to study the organization of matter at the microscopic level is not unprecedented; rather, optical trapping is now established as a valuable method for experimentalists in a diverse array of scientific fields, including molecular biology, biophysics, micro-rheology, and soft condensed matter physics.[1] The characterization of the optical trapping forces for single particles, classified as dipolar in nature,[2] became important and relevant as the instrument began to be implemented experimentally to measure small external forces, such as the mechanical properties of DNA, to evaluate systems with small thermal perturbations, such as biharmonic potentials, or to quantification of critical Casimir forces.[3] A thorough understanding of such single-particle optical forces has proven paramount to comprehending interactions within multi-particle arrays, such as those in self-organization studies.

One primary light-matter factor in optical traps is scattering.[4] Scattering is known to affect the strength of a trap, especially for high-refractive-index subjects,[5] but its parametric importance pales in comparison to that of the gradient force for single traps.[6] For inter-trap correlations, the redistribution of light from one trapped particle—particularly by scattering—to its neighbor(s) is much more significant. Optical scattering by individual microspheres has been shown to cause a phenomenon dubbed 'optical binding,' wherein the dispersed light impacts the ground state structural configuration of a collection of trapped particles.[7]

Also contributing to the nature of optical trap design and stability are interference-related effects. Retro-reflected light from a planar surface—like that from the interface between a glass microscope slide and an aqueous medium—can significantly alter the quality or Hookean stiffness of an optical trap when it interferes with the incident laser beam.[8] Moreover, interference effects can be used to dictate the orientation of a system of trapped colloidal particles in up to three dimensions; in one and two dimensions, overlapping and interfering laser beams can be used to study phase behavior in confined geometry.[9] Extended three-dimensional 'crystalline' structures can be formed and fully manipulated through interference effects.[10]

Perhaps of more interest are polarization-dependent optical trap characteristics, and their impact on dipole potentials. That lateral efficiency and stiffness of the trapping potential is dependent on the orientation of the linear polarization of the electric field is not a new idea; the concept has been predicted in numerical simulations,[11] and observed in several experiments.[12] This paper focuses on the behavior of silica microspheres in a multiple-Gaussian-beam optical tweezers setup, which utilizes a single objective lens to focus incident laser light; the setup implements an electronically-controlled steering mirror to modulate the trap position as a

function of time, allowing for the possible detection of polarization-dependent behavior between trapped spheres.

II. EXPERIMENTAL PROCEDURE

1. Experimental Setup

As mentioned above, a fully-steerable multiple-beam optical tweezers setup featuring electronically-controlled Gimbal mirrors was employed in this experiment to trap and dynamically manipulate colloidal microspheres. A schematic of the optical setup, which is based on a previously published design, is detailed in Figure 1.[13] Two Nd:YVO_4 lasers (Spectra-Physics Millennia Vs and Coherent DPSS 532-100, emitting light at a wavelength of 532 nm, were used to form the traps, so as to eliminate the possibility of interference between the multiple modes of the highly-coherent lasers.

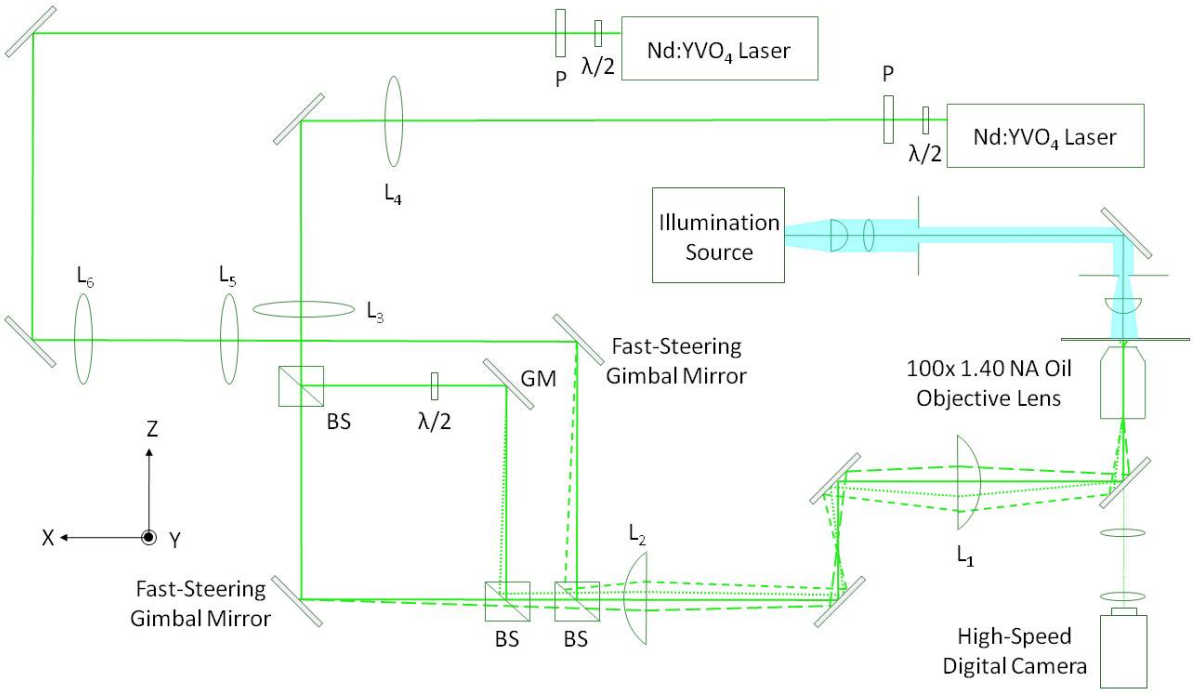

Figure 1: A schematic of the setup geometry as viewed from above. Note that in reality the imaging and illumination paths and the portion of the optical train from the periscope—between L_1 and L_2—to the objective are oriented vertically such that the objective is in an inverted-microscope configuration. The orientation of the coordinate system at the trap is shown at left: $+z$ is in the direction of beam propagation and gravity acts in the $-z$ direction (at the trap). Relevant optical components are shown: polarizers, P; half-wave plates, λ/2; Gimbal mirror,

GM; and non-polarizing cubic beamsplitters, BS.

The setup has three independently-steerable beams, two of which are electronically-controlled by fast-steering Gimbal mirrors (Newport FSM-300-01 mirror, Newport FSM-CD300B controller/driver). The power of the two parent beams can be manually tuned by adjusting the half-wave plates at the output of each laser, with the linear polarization preserved by coupling this waveplate with a polarizing prism (Newport 10GLO8AR.14). The third beam, formed by a non-polarizing cubic beamsplitter, can be manually manipulated with a Gimbal-mounted mirror and the orientation of its linear polarization can be controlled independently by a multiple-order half-wave plate (Tower Optical).

Trapped spheres were viewed through the microscope objective (Olympus PlanApo 100x, 1.40 NA oil immersion), with images being captured at up to 800 fps in uncompressed audio-video interleave (AVI) format by a digital camera (PixeLINK Monochrome Machine Vision Camera, PL-B741F). The image plane is illuminated homogeneously using a standard microscopy technique called Köhler illumination.[14]

2. Observation of behavior in line optical tweezers formed by a fast-steering mirror

The line optical tweezers has been demonstrated as a functional tool for measuring colloidal interactions and kinetics.[15] An electronically-controlled Gimbal mirror called a fast-steering mirror (FSM) was used to steer two of the beams in our optical setup, and was investigated as a means to create a line optical tweezers. The advantages of such a mirror are twofold: the beam can be guided in two dimensions (x and y in Figure 1), and a programmed function can be employed to dictate the local irradiance along the line by modulating the frequency of oscillation. By applying a high-frequency amplitude-modulated differential voltage to the Newport FSM, the physical tilt of the mirror responds accordingly and when steering a laser beam, forms what appears to be a linear-shaped optical potential. An optical trap formed in

this dynamic manner is much different in nature than a static line tweezers formed, for example, by a cylindrical or axiconical lens. Consider the line trap shown in Figure 2: if it were formed by a cylindrical lens, the nine trapped spheres would be in the direct path of the laser beam at all times; however, as is the case for this image, the line trap was formed by scanning a regular beam along the line at a frequency of 100 Hz—thus, ignoring the mechanical following error of the mirror, each of the nine spheres is trapped by the laser beam for approximately 1.1 ms every cycle. This temporal discontinuity of trapping at a given point contributes to complex observed behavior in two and three dimensional line traps.

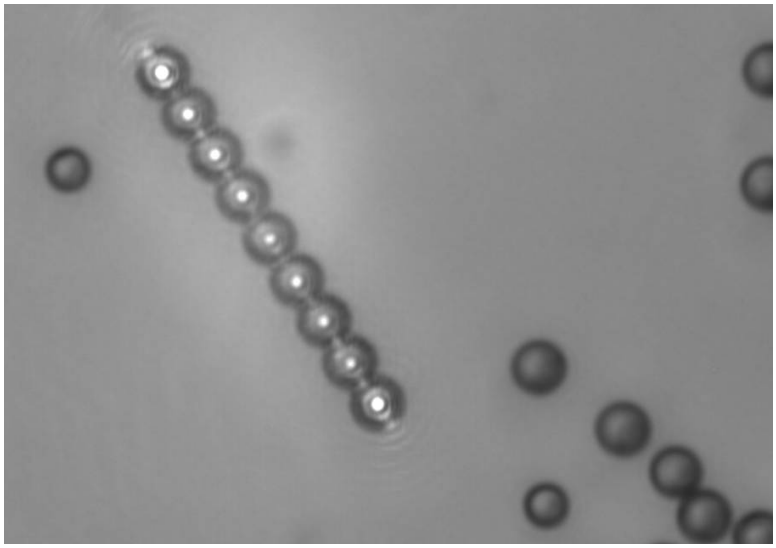

Figure 2: A line trap potential formed in two dimensions on the surface of a glass microcell by a fast-steering mirror (FSM). The line was formed by applying a 100 Hz sinusoidal function to the command inputs of a Newport FSM. The spheres shown are 4.38 ± 0.31 μm diameter carboxylated polystyrene microspheres (Polysciences, Inc.) in an aqueous solution, and the microscope objective used was a 100x lens with numerical aperture 0.55 (Mitutoyo, M PlanApo SL100).

A line optical tweezers was formed in a preliminary experiment upon the bottom surface of a borosilicate glass microcell (Vitrocom Vitrotubes, W5010-50), with the microscope objective oriented such that the beam propagated in the direction of gravity. In this configuration, carboxylated polystyrene spheres of diameter 4.38 ± 0.31 μm, 2.035 ± 0.045 μm (Polysciences, Inc.) were trapped in aqueous solution using a 100x, 0.55 NA microscope

objective (Mitutoyo, M PlanApo SL100). The spheres were easily trapped in 100-150 Hz sinusoidal lines with amplitude of up to ~60 μm as well as in other geometrical orientations of the optical potential (such as ellipses, circles, two parallel lines, and an un-modulated trap), all formed by a single beam steered by the FSM; however, these spheres were not trapped in the *z* direction—in each geometry, they could not be lifted from the surface—and for this reason a 40x objective with a higher 0.75 NA was used instead (Olympus, PlanApo), albeit with similar results. The optical configuration was modified further and a new type of sample cell prepared, as shown in Figure 3, with hopes of increasing the numerical aperture (and therefore the restoring gradient force) as well as decreasing aberrations caused by the sample cell; this sample cell concept was used for all further experimentation.

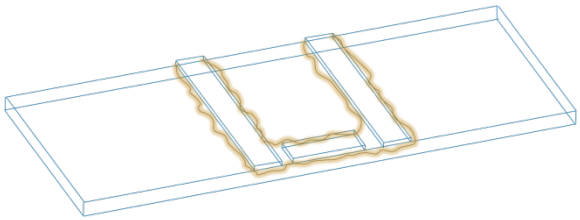

Figure 3: A typical sample cell prepared from a standard microscope slide. The three walls at the boundaries of the cell are made by scoring and breaking a No. 2 coverslip and are secured to the slide with a five-minute two-part epoxy. A No. 2 coverslip is then secured to the top of this with the same epoxy. Upon filling the cell, it is sealed with a silicone caulking compound.

Even with this new cell, featuring more planar surfaces, and a 100x oil immersion objective (Olympus PlanApo, 1.40 NA) installed, a three-dimensional trap was attempted with the aforementioned polystyrene spheres as well as with 2.35 μm and 0.60 μm silica microspheres (Bangs Laboratories, Inc.). Such a trap was unachieved, and the reason is that both maximum axial and transverse trapping efficiency are well-known to dramatically decrease as the trap is moved further from the cover glass, and in the setup just described, the attempted trapping location—at the bottom of the cell—was at a distance of no less than 100 μm from the cover glass.[16] Hence, the optical setup was reconfigured to the inverted microscope orientation

described in Figure 1. This change permitted trapping of single particles in both two and three dimensions, as expected, but surprisingly did not facilitate two or three dimensional trapping of polystyrene or silica spheres.

A very noticeable difference in trapping behavior existed between the upward-propagating (against gravity) and downward-propagating (with gravity) orientations of the tweezers; the two setup designs are represented in Figure 4.

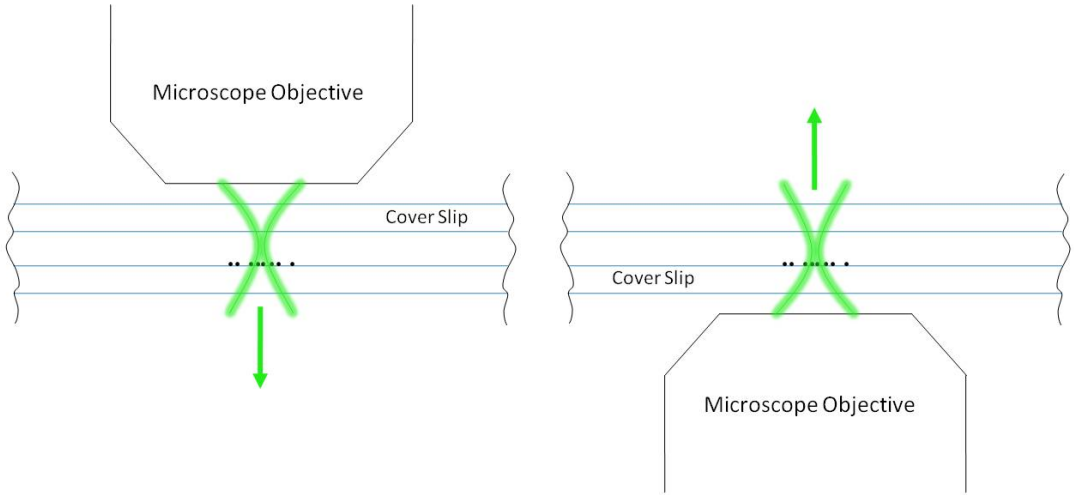

Figure 4: Left: Original orientation of the microscope objective, in which the laser propagated in the direction of gravity. Right: Final inverted orientation of the microscope objective, in which the laser beam was against gravity. In this final setup, the slide shown in Figure 3 was flipped so that the distance to the trapped spheres beyond the coverslip was minimized. The depth of the cell was approximately the thickness of the coverslip, or 0.17 mm.

In a line trap formed in the downward-propagation configuration, a single trapped sphere was uninfluenced by the position of the laser beam, and therefore uninfluenced by any frequency modulation of the voltage applied to the FSM; i.e., the spheres did not follow the oscillations of a beam beyond 20 Hz. However in the inverted orientation, in addition to being much more difficult to trap in a line-shaped potential, any trapped spheres were shown to follow the position of the oscillating beam to relatively high frequencies. Clearly, a change in the way the spheres were confined occurred with this change of orientation that considerably changed trapping behavior.

A simple test was devised to determine at what increased frequency, if any (within the safe operating limits of the Newport FSM), the spheres stopped following the moving beam, becoming insensitive to the dynamic nature of the potential. Phase-locked 93.000 Hz sinusoidal signals were applied to each axis of the FSM, such that the position of the trap traced out a circle in the image (*x*-*y*) plane. A single 0.60 μm sphere was trapped and imaged at 400 fps; frame-by-frame playback revealed that upon each pass of the beam, the sphere was given a large impulse such that its average angular velocity was constant. With 400.000 Hz sinusoidal signals on both FSM command inputs, near the upper operational limit for the 0.0700 V_{pp} amplitude used, phase slips in the particle's motion were observed; i.e., occasionally a pass of the beam imparted a significantly smaller impulse, resulting in intermittent pauses in its progression around the circular path. These observations imposed the constraint that the FSM be operated at very low frequencies in order to ensure predictable motion of the trap and guarantee that any behavior observed in the polarization experimentation discussed below was not caused by dynamic effects of the mirror.

3. Observation and measurement of polarization effects

Before any polarization-dependent interactions between trapped spheres can be measured, they must first be definitively witnessed. Polarization has been shown to have dramatic consequences for trapping and inter-particle behavior in anisotropic fluids like liquid crystals, particularly due to the strong interaction between the electric field and the medium.[17] In an isotropic aqueous trapping medium however, one does not expect a strong impact of the polarization of incident laser light on the medium, in part because the polarity of water molecules cause them to strongly interact with each other instead of with a pervading electric field. The degree of any polarization effect will not be magnified by an aqueous medium, and because it

will depend on the magnitude of the dipole field induced, will be quite small. One might expect, since trapped particles behave like dipoles, that orthogonally-oriented dipoles (corresponding to orthogonal polarization) will not interact as strongly as those that are parallel-oriented (due to parallel polarization). A dynamic detection method was employed to investigate this notion; a single 0.6 μm silica sphere was maintained in a fixed position with fixed linear polarization as the spatial proximity of an adjacent trapped sphere was varied sinusoidally at a rate of 0.05 Hz with an amplitude of 1110 ± 120 nm (see Figure 5), with the intent that any attraction or repulsion by polarization effects would be visualized by extracting the 0.05 Hz signal from the fluctuations in the position data for the unmodulated particle. In the event that a signal was present in the 'stationary' particle as well, the difference in the magnitudes of these signals—perhaps found by performing a fast Fourier transform (FFT)—could be used as an indicator of any difference between the parallel and orthogonal polarization states.

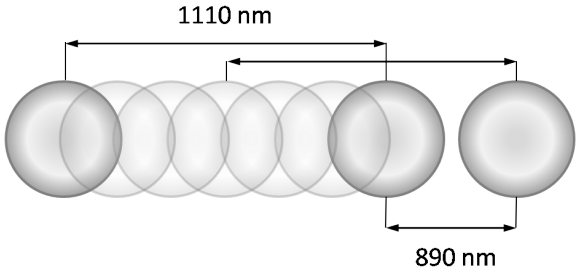

Figure 5: Configuration for dynamic probe of polarization-based interactions between trapped silica spheres. Two 0.6 μm spheres were used: the sphere on the right was held in a fixed location with fixed linear polarization. The sphere at left was manipulated using a 0.05 Hz sine function as close as 890 nm from the fixed sphere and as far as 2000 nm. The amplitude of the oscillation was therefore 1110 nm (uncertainty of 120 nm).

Metric distances at the trap were determined by a micron-to-pixel ratio of 0.04. This scheme, first with parallel and then with orthogonal polarization, was captured via digital camera with a total of 6000 frames at 600 fps for each data run.

III. ANALYTICAL PROCEDURE AND DISCUSSION OF RESULTS

The positions of both spheres were recovered from the AVI files using a particle-tracking algorithm (ImageJ particle detector and tracker plug-in).[18] The position of the particles in the axis of motion was plotted, and because of the level of noise, a FFT was performed on the position data to look for any dominant frequencies; i.e. the 0.05 Hz modulation frequency and/or its harmonics (see Figure 6).

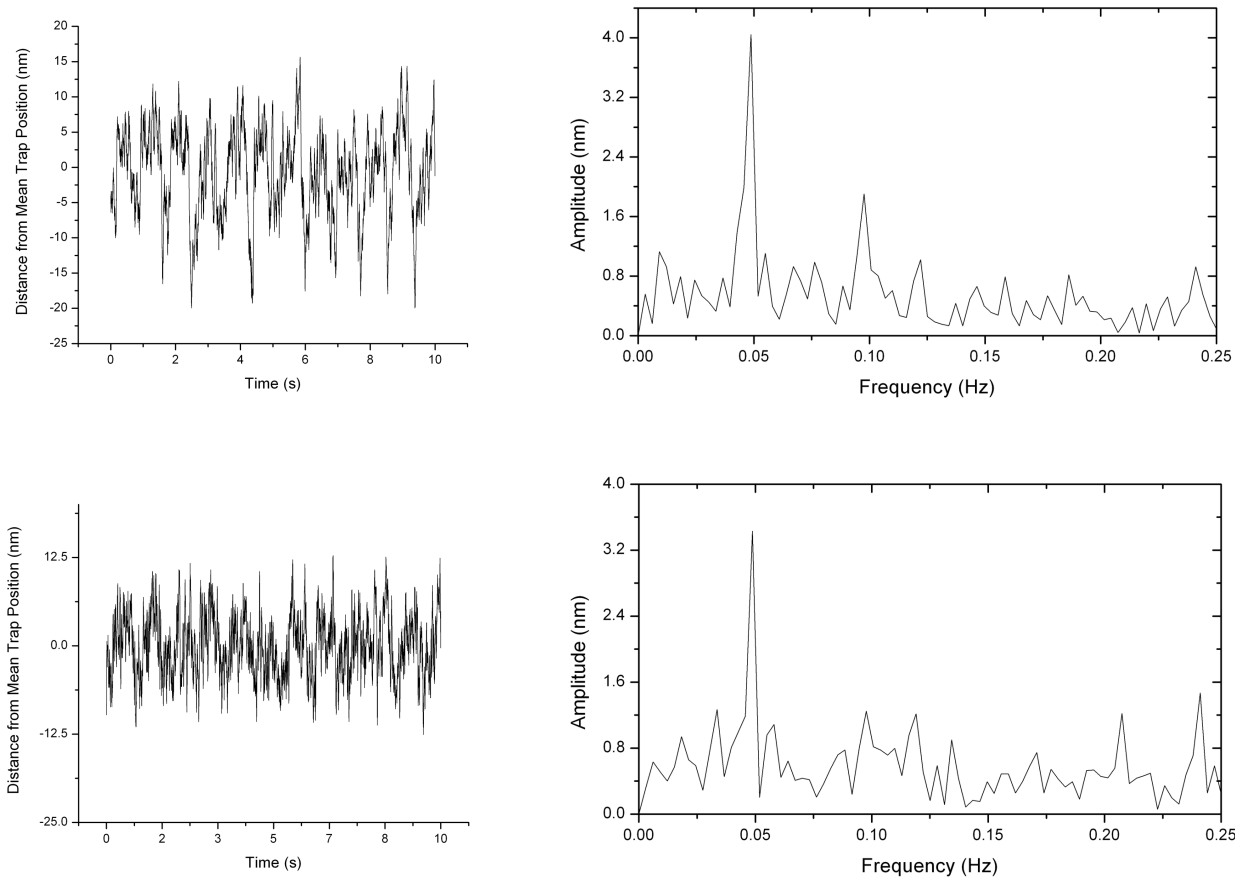

Figure 6: Position data in the axis of interest for the parallel and orthogonal polarization cases and corresponding FFTs. Top left: The position of the particle in the fixed trap, plotted as the distance from the mean trap position vs. time, for the parallel polarization case. Top right: The FFT corresponding to the graph at top left. Bottom left: The position of the particle in the fixed trap, plotted as the distance from the mean trap position vs. time, for the orthogonal polarization case. Bottom right: The FFT corresponding to the graph at bottom left.

The fluctuations in position of both particles indeed contained a strong 0.05 Hz component, suggesting that the moving trapped particle had some kind of effect on the position of the sphere in the stationary trap. Unfortunately, the difference between the magnitudes of these peaks is within the noise in the FFT graph. To determine whether the distinction is the result of a polarization effect, the number of data points plotted should be increased, as it would improve the frequency resolution and decrease the magnitude of the relative noise in the FFT plot.

More information is necessary regarding the dependence of these observed results on trapping power and the shape of the potentials before the effect can be definitively isolated as a polarization-determined behavior. For example, knowing how the stiffness of the overall potential changes as the two traps become closer together—and overlap significantly—would shed further light on the source of the effect shown in Figure 6. Additionally, verification that this setup is sensitive enough to detect the asymmetry in transverse stiffness due to linear polarization would determine the extent to which the methodology we used is capable of measuring tiny forces. Another factor to consider is that the physical rotation of a waveplate to alter the relative polarization of the beams can introduce a slight translation of the waveplate, possibly introducing a systematic error that could be falsely attributed to polarization-dependent particle interactions.

IV. SUMMARY AND CONCLUSION

Prior research has shown that the axial and transverse stiffness/trapping efficiency for optically-tweezed particle are asymmetric; in this experiment, these concepts were extended in an exploration of the polarization-related influences between optically-trapped colloidal microspheres. An adapted multiple-beam steerable optical tweezers setup was used, featuring electronically-powered fast steering mirror. Before exploring the possibility of polarization-

dependent behavior, the limitations of this steering mirror were investigated to ensure that the mirror could be ruled out as a potential factor in any observed interactions between trapped particles.

Treating two trapped particles as dipoles, their interaction was investigated with respect to polarization-related causality. A silica sphere trapped in a fixed beam was shown to exhibit small sinusoidal fluctuations in response to the movement of an adjacent trapped particle, and the amplitude of these fluctuations, yet additional data is necessary to isolate this behavior as being truly polarization-dependent.

ACKNOWLEDGEMENTS

Aaron would like to thank Dr. Brage Golding (Michigan State Univ., Dept. of Physics & Astronomy) and Dr. Lowell McCann (Univ. of Wisconsin-River Falls, Dept. of Physics) for facilitating my role in this project as a part of Michigan State University's Research Experience for Undergraduates (REU) Program, as well as for their effort to make the experience an outstanding learning opportunity. Sponsorship for this research was graciously provided by the National Science Foundation.

[1] A. Ashkin, J. Dziedzic, J. Bjorkholm, and S. Chu, Opt. Lett. **11** (5), 288-290, (1986); D. G. Grier, Curr. Opin. Colloid Interface Sci. **2**, 264–270 (1997); A. Ashkin, Proc. Natl. Acad. Sci. U. S. A. **94**, 4853–4860 (1997).
[2] T. Tlusty, A. Meller, and R. Bar-Ziv, Phys. Rev. Lett. **81** (8), 1738-1741 (1998).
[3] U. F. Keyser, J. van der Does, and N. H. Dekker, Rev. Sci. Instrum. **77** 105105 (2006); L. I. McCann, M. Dykman, and B. Golding, Nature **402** (6763), 785-787 (1999); C. Hertlein, et al., Nature **451** (10), 172-175 (2008).
[4] A. Ashkin and J. M. Dziedzic, Appl. Opt. **19** (5), 660-668 (1980); A. Ashkin and J. M. Dziedzic, Appl. Opt. **20** (10), 1803-1814 (1981).
[5] V. Bormuth, et al, Opt. Express **16** (18), 13831 (2008).
[6] A. Ashkin, J. Dziedzic, J. Bjorkholm, and S. Chu, op. cit. 288-290.
[7] N. K. Metzger, K. Dholakia, and E. M. Wright, Phys. Rev. Lett. **96** (6), 068102-1 (2006); N. K. Metzger, E. M. Wright, W. Sibbett, and K. Dholakia, Opt. Express **14** (8), 3677-3687 (2006).
[8] P. Jákl, et al., J. Opt. A: Pure Appl. Opt. **9**, S251-S255 (2007).
[9] C. Bechinger and E. Frey, J. Phys.: Condens. Matter **13**, R321–R336 (2001).
[10] M. P. MacDonald, et al., Science **294**, 1101 (2002).
[11] A. R. Zakharian, P. Polynkin, M. Mansuripur, and J. V. Moloney, Opt. Express **14** (8), 3660-3674 (2006).
[12] Y. Roichman, B. Sun, A. Stolarski, and D. G. Grier, Phys. Rev. Lett. **101**, 128301 (2008); A. Rohrbach, Phys. Rev. Lett. **95**, 168102 (2005); D. Ganic, X. Gan, and M. Gu, Opt. Express **12** (12), 2670-2675 (2004); W. H. Wright, G. J. Sonek, and M. W. Berns, Appl. Opt. **33** (9), 1735-1748 (1994).
[13] E. Fällman and O. Axner , Appl. Optics **36** (10), 2107-2113 (1997).

[14] S. Inoué and K. R. Spring, *Video Microscopy, The Fundamentals* (Plenum Press, New York, 1997), 2nd ed., pp. 13-26, 119-130.
[15] P. L. Biancaniello and J. C. Crocker, Rev. Sci. Intsrum. **77**, 113702 (2006).
[16] D. Ganic, et al., op. cit., 2674.
[17] I. I. Smalyukh, A. V. Kachynski, A. N. Kuzmin, and P. N. Prasad, PNAS **103** (48), 18048-18053 (2006).
[18] I. F. Sbalzarini and P. Koumoutsakos, J. Struct. Biol. **151** (2),182-195 (2005).